

Published in final edited form as:

J Nucl Med. 2009 August ; 50(8): 1356–1363. doi:10.2967/jnumed.108.060822.

Serial Non-Invasive Targeted Imaging of Peripheral Angiogenesis: Validation and application of a semi-automated quantitative approach¹

Lawrence W. Dobrucki¹, Donald Dione¹, Leszek Kalinowski¹, Donna Dione¹, Marivi Mendizabal⁴, Jun Yu², Xenophon Papademetris¹, William C. Sessa², and Albert J. Sinusas¹

¹Department of Internal Medicine, Section of Cardiovascular Medicine, Yale University School of Medicine, New Haven, Connecticut, U.S.A ²Department of Pharmacology, Yale University School of Medicine, New Haven, Connecticut, U.S.A ³Department of Clinical Chemistry and Biochemistry Medical University of Gdansk, Gdansk, Poland ⁴GE Healthcare, Buckinghamshire, UK

Abstract

Previous studies by our group have demonstrated the feasibility of non-invasive imaging of α_v integrin to assess temporal and spatial changes in peripheral and myocardial angiogenesis. In this study we validate the reproducibility, accuracy, and applicability of a new semi-automated non-invasive approach for serial quantitative evaluation of targeted microSPECT-CT images of peripheral angiogenesis in wild-type and eNOS-deficient mice subjected to hindlimb ischemia.

Methods—Mice (n=15) underwent surgical ligation of the right femoral artery to induce unilateral hindlimb ischemia. One week post ligation, a ^{99m}Tc-labeled cyclic-RGD peptide targeted at α_v integrin (NC100692, n=10) or a ^{99m}Tc-labeled negative control (AH-111744, n=5) was injected and 60-min later *in vivo* microSPECT-CT images were acquired. Mice were euthanized, tissue from proximal and distal hindlimb was excised for gamma well counting (GWC) of radiotracer activity, and ischemic-to-nonischemic (I/N) ratio calculated. MicroSPECT-CT images were analyzed using a new semi-automated approach which applies complex VOIs derived from segmentation of the microCT onto microSPECT images to calculate I/N activity ratios for the proximal and distal hindlimb. Studies were reprocessed for determination of intra- and inter-observer variability.

To compare 3D VOI analysis with traditional manual 2D ROI analysis of maximum intensity projection images, microSPECT images were summed onto a single anterior-posterior projection. Rectangular ROIs were manually drawn and I/N ratio calculated.

Our new 3D analysis approach was applied to additional groups of mice (eNOS^{-/-}, n=5; wild-type, n=3) imaged before, 1 and 4 weeks after femoral artery resection.

Results—Our new semi-automated approach for evaluation of α_v integrin targeted microSPECT-CT images demonstrated both a high intra- and inter-observer variability ($R^2=0.997$), and accuracy ($R^2=0.780$) for estimation of relative radiotracer activity relative to GWC. Analysis of serial microSPECT-CT images demonstrated a significant increase in relative

¹Short running title: “Quantitative Imaging of Peripheral Angiogenesis”

Address for correspondence: Albert J. Sinusas, MD, Professor of Medicine and Diagnostic Radiology, Section of Cardiovascular Medicine, Yale University School of Medicine, P.O. Box 208017, 3FMP, New Haven, CT 06520-8017, Phone: (203) 785-4915, Fax: (203) 785-4007, albert.sinusas@yale.edu.

First author: Lawrence W. Dobrucki, PhD, Postdoctoral Fellow, Section of Cardiovascular Medicine, Yale University School of Medicine, BML 324, New Haven, CT 06520, Phone: (203) 785-4909, Fax: (203) 785-4007, wawrzyniec.dobrucki@yale.edu

NC100692 retention in the ischemic hindlimb of both wild-type and eNOS-deficient mice at 1 week after surgery. There was a significant (~25%) decrease in radiotracer uptake in eNOS^{-/-} mice relative to wild-type animals, which was not observed at baseline or 4 weeks post ligation.

Conclusion—A new semi-automated analysis of αv integrin targeted microSPECT-CT images provides a non-invasive approach for serial quantitative evaluation of peripheral angiogenesis. The reproducibility and accuracy of this approach allows for quantitative analysis of serial targeted molecular images of lower extremities, has applicability to other targeted SPECT or PET radiotracers, and may have implications for clinical imaging in patients with PAD.

Keywords

molecular imaging; microSPECT; microCT; peripheral angiogenesis

Introduction

The introduction of genetic and cell based therapies along with nanoparticle drug delivery systems for treatment of cardiovascular diseases through stimulation of angiogenesis has motivated the development of non-invasive imaging approaches to evaluate and track the response to these therapies. Angiogenesis is a complex process that involves many stimuli, growth factors and interactions between multiple cell types. A number of experimental models have been developed to evaluate this process and novel therapeutic interventions in normal and transgenic mice. The experimental evaluation of peripheral angiogenesis traditionally has relied on assessment of the pathological and physiological changes associated with the angiogenic process, using well established models of hindlimb ischemia to define the molecular events associated with angiogenesis. The genetic loss of endothelial NOS was found in models of hindlimb ischemia to impair vascular endothelial growth factor (VEGF) signaling, ischemia-induced angiogenesis and blood flow recovery, and was associated with limb necrosis.¹ These mechanistic studies of the angiogenic process generally require the euthanasia of animals at selected time points because of the application of highly invasive measures or tissue analyses. A number of investigators have demonstrated the feasibility of non-invasively evaluating angiogenesis using image-based approaches targeted at cell surface receptors that are upregulated and/or activated in association with the angiogenic process.²⁻⁷

Peptides containing the tripeptide sequence RGD (Arg-Gly-Asp) are known to bind with a high affinity to the αv integrins associated with angiogenesis. Investigators have reported use of radiolabeled tracers containing RGD motif for non-invasive imaging of angiogenesis in different animal models.⁸⁻¹¹ A ^{99m}Tc-labeled cyclic RGD peptide (^{99m}Tc-NC100692, GE Healthcare, UK) targeted at αv integrins was demonstrated to provide efficacy and safety of imaging malignant breast tumors.⁸ More recently, Edwards et al. demonstrated that NC100692 had a high affinity for the αv integrins, was metabolically stable and had a biodistribution favorable for *in vivo* imaging purposes.⁹

We previously demonstrated the potential of planar gamma camera imaging with ^{99m}Tc-NC100692 for evaluation of spatial and temporal changes in peripheral angiogenesis in mice subjected to hindlimb ischemia.⁵ This previous study demonstrated a positive correlation between quantitative analysis of planar images of NC100692 and gamma well counting of tissue specimens, although the analysis of *in vivo* planar pinhole images tended to underestimate the magnitude of the relative increases in NC100692 retention within the ischemic hindlimb. We hypothesized that these differences might be due to attenuation and partial volume errors, as well as selection of inappropriate regions of interest, and that images could be more accurately quantified by use of a high-resolution hybrid

microSPECT-CT imaging system that would provide anatomical localization of the targeted radiotracer within the intended tissues.

In the current study we describe a new non-invasive approach for serial quantitative evaluation of radiotracers targeted at α_v integrins in established models of hindlimb ischemia for evaluation of ischemia-induced angiogenesis. Initial studies were performed to develop and validate the accuracy and reproducibility of a semi-automated image analysis approach. Additional studies were performed to non-invasively define the temporal changes in angiogenesis in control mice and eNOS-knockout (eNOS^{-/-}) mice in response to ischemic injury using our quantitative hybrid microSPECT-CT α_v integrin targeted imaging approach. Quantitative analysis of microSPECT-CT images of α_v integrins and other targeted biological markers will be critical for understanding the angiogenic process and tracking novel molecular or genetic therapies applied to models of hindlimb ischemia, and may have implications for evaluation of patients with peripheral arterial disease.

The method proposed here can be applied to quantify SPECT-CT or PET-CT images of virtually any radiotracer within limbs of animals or patients, and represents an important step in standardizing the quantification of nuclear images of the peripheral limbs.

Materials and Methods

Overview of Surgical Model and Experimental Protocol

All experiments were performed according to the guiding principles of the American Physiological Society and approved by the Institutional Animal Care and Use Committee. Male C57BL/6 mice (Charles River Laboratories, Wilmington, MA) were anesthetized with 1-3% isoflurane for surgical intervention and imaging. For initial methodological development and validation of the α_v integrin targeted microSPECT-CT imaging approach, a subset of mice (n=15) underwent sterile surgical occlusion of the right femoral artery to induce unilateral hindlimb ischemia according to the modified procedure described previously.⁵ The surgical model employed in the initial validation studies resulted in a very small post-operative wound with minimal inflammation. These mice underwent α_v integrin targeted microSPECT-CT imaging at 7 days after surgery, a time point previously established to correspond with maximal activation of the α_v integrins.⁵ For further application of the developed quantitative approach for non-invasive serial imaging of angiogenesis, additional wild-type (eNOS^{+/+}, n=3) and eNOS^{-/-} mice (n=5) underwent sterile surgical removal of left femoral artery to induce severe unilateral hindlimb ischemia, using a surgical approach previously described.¹ Before each imaging session, a PE-10 catheter was placed into right jugular vein for radiotracer injections.

MicroSPECT-CT Imaging Protocol

For the validation studies, all animals (n = 15) were injected intravenously with ~37 MBq of either the ^{99m}Tc-labeled chelate-peptide conjugate containing an RGD (Arg-Gly-Asp) motif (^{99m}Tc-NC100692, n=10) targeted at the α_v integrin or a negative control scrambled peptide (^{99m}Tc-AH-111744-01, n=5) 7 days after surgical induction of hindlimb ischemia. Imaging was performed with a hybrid dual-headed microSPECT-CT small animal scanner (X-SPECT, GammaMedica-Ideas, Northridge, CA) equipped with 1-mm pinhole collimators. Animals were placed on the animal bed in the supine position with legs secured in an extended position. 60 min after radiotracer injection, mice underwent SPECT imaging (32 projections, 60 sec/projection per head) with a 20% energy window centered at 140 keV. This was followed by high resolution anatomical CT imaging (512 projections, 50kVp/600 μ A energy). Mice were euthanized immediately after CT imaging was completed and soft tissue samples from both legs were taken for gamma well counting. For serial imaging

studies, animals (n=8) were injected intravenously with ~37 MBq of ^{99m}Tc -NC100692 before and after 1 and 4 weeks of hindlimb ischemia and imaged according to the protocol described above.

MicroSPECT-CT Image Reconstruction and Analysis – Validation Studies

Image Reconstruction and Analysis—The microSPECT and microCT images were reconstructed using existing commercial software (X-Flex, GammaMedica-Ideas and Cobra Exim, respectively). MicroSPECT images were filtered (Butterworth, cut-off $0.5 \times$ Nyquist frequency and order of 6), fused with microCT images and converted to Analyze format (Mayo Foundation). The relative uptake of targeted tracer within the soft tissue of the hindlimbs was quantified using semi-automated software developed as part of the current study and now available online (<http://www.bioimagesuite.org/>). Complex irregular volumes of interest (VOIs) were generated from the microCT images as described below and registered with the microSPECT images. These complex regions included only soft tissue structures from the hindlimb with skeletal structures removed from the image during the segmentation process described below.

To compare our semi-automatic volumetric quantification of 3D microSPECT images with more traditional 2D analysis of planar or maximum intensity projection nuclear images, microSPECT images were summed onto a single anterior-posterior projection and rectangular 2D ROIs were manually drawn on the maximum intensity projection image. The mean counts from each 2D ROI within ischemic hindlimb were calculated and normalized to the contralateral ROIs drawn on non-ischemic hindlimb and expressed as ischemic-to-non-ischemic (I/NI) ratio.

For 3D volumetric image analysis, microCT images were loaded into our image analysis tool and visualized as a semi-translucent [?] 3D rendering. The microCT image intensity was adjusted by the operator to optimally visualize the skeletal and muscular structures. The operator positioned eight planes (4 on each side) to segment the microCT image of a mouse into 7 regions including; main thorax with the tail, left proximal and distal hindlimb, and left foot, right proximal and distal hindlimb, and right foot. Two planes were used to define each hip joint, one axial above the femur and one sagittal at the pelvic joint. The knee was axially bisected between the femur and tibia. A final plane was used at ankle joint to separate the foot. After the planes were positioned, automatic K-means clustering-based segmentation removed the bone from the microCT image. [ref] A seven-region segmentation image or “objectmap” (an integer-valued image in the range 0..7 where the labels 1-7 were used to identify the 7 regions) was automatically created excluding the skeleton from the VOIs (Figure 1). This objectmap was then applied to the corresponding microSPECT images to determine mean counts in each VOI. The radiotracer activity from the ischemic proximal and distal hindlimb was normalized by the contralateral non-ischemic proximal and distal hindlimb respectively, in order to compute I/NI ratio.

Image Analysis Versus Gamma Well Counting—To validate the accuracy of the quantitative non-invasive targeted imaging approach, image derived results from our new 3D VOI and traditional 2D ROI analysis were compared with gamma well counting of the corresponding tissue samples. The soft tissues in hindlimbs were excised, excluding the bones, and divided into proximal and distal sections according to the position of the major joints. The tissue samples were weighed, and the ^{99m}Tc activity was measured using gamma well counter (Cobra Packard) and corrected for background, decay time, and tissue weight. The corrected counts from the proximal and the distal hindlimbs were used to calculate the I/NI ratios for each mouse. The registered microSPECT and microCT images and CT-derived

VOIs were qualitatively inspected for background activity that might have scattered into the VOIs from adjacent non-muscular structures, such as the bladder.

Intra- and Inter-observer Variability—The intra- and inter-observer variability was assessed to determine the reproducibility of this quantitative analysis. For intra-observer variability, fused microSPECT-CT image sets were analyzed twice by a single operator. The time interval between the two reading studies varied between few hours to a couple of days. To define the inter-observer reproducibility of the analyses, fused microSPECT-CT image sets were analyzed by two different operators. The results were expressed as I/NI ratio in distal hindlimb and statistically analyzed using a paired student T-test. For the correlation between different analyses the Pearson correlation coefficients were calculated.

Serial microSPECT/CT Imaging of Peripheral Angiogenesis – Application Studies

The image analysis approach was applied to an additional series of images acquired before and after femoral artery occlusion, to monitor peripheral angiogenesis in wild-type and eNOS $-/-$ mice subjected to severe hindlimb ischemia. The serial microSPECT and microCT images acquired at baseline, and 1 week and 4 weeks post femoral occlusion were reconstructed, fused and converted for analysis as outlined above. The relative uptake of the targeted radiotracer in the distal hindlimb was computed by a single operator. The I/NI ratio of activity within the distal hindlimbs were compared using ANOVA followed by a paired Student-t test.

Results

Validation of Image Analysis Approach

To evaluate the accuracy of our quantitative image analysis approach, the image-derived I/N activity ratios from both proximal and distal hindlimbs were plotted against corrected ratios derived by gamma well counting of tissue. This initial analysis demonstrated a very poor correlation ($R^2=0.05$) between the quantitative image-derived results and gamma well counting (Figure 2A). However, we identified animals ($n=5$) in which there was evidence of significant scatter into the proximal segments from highly radioactive urine within the animal's bladder. This scatter resulted in a variable overestimation of counts in the proximal hindlimb from image analysis. After excluding those mice from the analysis with clear contamination of the proximal VOIs, the correlation coefficient between the quantitative image analysis and gamma well counting was excellent (Figure 2B), with a significantly improved correlation coefficient ($R^2=0.63$). Figure 2C shows a representative microSPECT image of an animal with radioactivity within the bladder which was positioned toward the proximal limb and encroaching into the proximal VOI of the ischemic hindlimb. In the majority of animals the bladder did not affect the quantitative image analysis of proximal sections. Figure 2D shows a microSPECT image of the animal with the radioactive bladder located centrally with no appreciable effect on image-derived activity from the proximal VOIs. To eliminate the scatter of activity within the bladder into the proximal VOIs we aspirated the urine from the bladder using a 30-gauge needle immediately before the microSPECT scan. Figure 2E shows a representative microSPECT image from a mouse following removal of the radioactive urine immediately before initiation of the microSPECT acquisition. Although this approach can potentially improve image quantification of proximal VOIs, this intervention may not be applicable for repeated serial imaging of animals over a prolonged period of time. In the majority of the mice analyzed, the bladder did not affect the image analysis.

The specificity of $^{99m}\text{Tc-NC100692}$ uptake toward α_v integrin was validated by use of $^{99m}\text{Tc-AH-111744-01}$, a negative control radiotracer containing a scrambled peptide.

Gamma well counting analysis of muscles from the distal leg demonstrated significant increase in the I/N ratios in ^{99m}Tc -NC100692-injected animals (2.10 ± 0.29 , $n=5$) relative to the negative control group (1.20 ± 0.28 , $n=5$, $P < 0.05$).

Our previous studies confirmed that the angiogenic response is seen primarily in the muscles of the distal leg¹². Due to this fact the subsequent validation studies were performed using results obtained from only the distal hindlimb. The accuracy of our 3D volumetric and traditional 2D approaches were evaluated by comparing the calculated I/N ratios from distal 3D VOIs and 2D ROIs with the results derived from corrected gamma well counting ratios. The results for the distal hindlimb are summarized in Figure 3. The quantitative image analysis was highly correlated with gamma counting, yielding a high correlation coefficient ($R^2=0.78$) for both 3D VOI and 2D ROI analysis. The residuals plot for both methods confirmed the quality of the fit. Although the correlation coefficients obtained using our new 3D volumetric and traditional 2D analysis method are similar, there was a significant underestimation of counts quantified using 2D ROIs (Figure 3C). The intra-observer (Figure 4A) and inter-observer (Figure 4B) variability of our 3D volumetric analysis were excellent as reflected by the very high correlation coefficients ($R^2=0.997$).

Serial microSPECT/CT Imaging of Peripheral Angiogenesis

MicroSPECT-CT images at 60 minutes after injection of ^{99m}Tc -NC100692 were of excellent quality and allowed for quantitative analysis of radiotracer retention in the ischemic distal limb. Figure 5A shows representative microSPECT-CT images recorded in wild-type and eNOS-knockout mice at baseline, 7 days and 4 weeks after femoral artery resection. Differences in the image-derived ratios of radiotracer retention (I/N) are shown in Figure 5B. A significant ($P < 0.05$) increase in ^{99m}Tc -NC100692 relative retention was observed in both wild-type (3.81 ± 0.60) and eNOS $-/-$ mice (2.85 ± 0.43) at 7 days from the onset of ischemia. Moreover, there was a significant ($\sim 25\%$) decrease in relative radiotracer retention in ischemic distal hindlimb of eNOS-knockout mice compared to wild-type animals ($P < 0.05$) suggesting an impairment of the angiogenic response at this time point. At baseline and 4 weeks after femoral artery resection there were no significant differences in relative ^{99m}Tc -NC100692 retention in the ischemic distal hindlimb between the wild-type (baseline: 1.47 ± 0.27 , 4 wks: 2.15 ± 0.79) and eNOS $-/-$ mice (baseline: 1.25 ± 0.58 , 4 wks: 2.14 ± 0.29 , $P = \text{NS}$).

Discussion

The experimental evaluation of spatial and temporal changes in peripheral angiogenesis is traditionally done using highly invasive techniques that require the collection and often the destruction of tissue samples, which prohibits serial monitoring of this biological process in living animal. We demonstrated the feasibility of serial ^{99m}Tc -NC100692 microSPECT-CT imaging for the noninvasive monitoring of ischemic induced angiogenesis *in vivo* using an established murine model of hindlimb ischemia. Applying this targeted imaging approach we were also able to confirm the previously observed early impairment of angiogenesis following ischemic injury in transgenic mice in which eNOS expression was reduced. To specifically target proliferating angiogenic vessels we used a ^{99m}Tc -labeled RGD peptide targeted to α_v integrins known to be activated during initiation of the angiogenic process. The specificity of the binding of the RGD peptide for activated endothelial cells was previously demonstrated using a fluorescein-labeled negative control compound containing a scrambled peptide.⁵ In this study we have confirmed the specificity of the RGD peptide using a ^{99m}Tc -labeled negative control compound (AH-111744-01) containing a scrambled peptide.

The novel noninvasive imaging approach for the quantitative serial assessment of angiogenesis in mice became possible with the development of targeted radiotracers like ^{99m}Tc -NC100692, as well as the development of dedicated small animal imaging systems. Among different imaging modalities both PET and SPECT are currently highly suited for molecular targeted imaging of biological processes, including angiogenesis, because of the relatively high sensitivity and capability for 3D imaging and quantification. The advantages and disadvantages of these two modalities have been described in detail in previously published reviews¹³⁻¹⁶. Briefly, PET provides higher sensitivity and more established attenuation correction algorithms. On the other hand SPECT generally provides better spatial resolution than PET for small animal imaging, and allows for the use of multiple isotopes simultaneously. The recently introduced hybrid imaging systems combining anatomical (CT, MRI) with functional (PET, SPECT) imaging allow for more accurate definition of ROIs or VOIs, and partial volume and attenuation corrections, which are important steps in standardizing the quantification of small animal nuclear images.

In this study the lower-resolution high-sensitivity microSPECT images were reconstructed and fused with the registered high-resolution anatomic microCT images for quantitative analysis. The analysis was based on CT segmentation of murine hindlimbs, definition of 3-dimensional VOIs and calculation of ischemic-to-nonischemic (I/NI) activity ratio from the microSPECT images. Our image derived quantitative analysis of relative radiotracer retention was validated with gamma well counting of tissue samples, an established “gold-standard” technique. We found a strong positive correlation ($R^2 = 0.78$) between relative (I/NI) retention of radiotracer assessed by image analysis and the gamma well counting in sections from the lower hindlimb distal the femoral occlusion. We compared our semi-automated 3D volumetric approach with more traditional manually defined 2D ROIs on planar equivalent maximum project nuclear images. Although the comparison of these two approaches with gamma well counting analysis resulted in similar correlation coefficients, we observed that 2D analysis tends to underestimate the counts derived from radiotracer uptake (Figure 3C). This phenomenon was observed and described in our previous studies by Hua et al {Hua, 2005 #20}. We hypothesized that this underestimation could be partially due to the selection of inappropriate ROIs and we proposed that the images could be more accurately quantified by using hybrid microSPECT-CT imaging which allows for anatomical localization and definition of 3D VOIs. Indeed, our 3D volumetric approach significantly improved the counts derived from ischemic hindlimb (Figure 3A). Manual definition of ROIs or VOIs by the operator introduces variability and a potential bias to the analysis. In contrast our approach is based strictly on definition of VOIs using anatomical landmarks including lower extremity joints and skeletal structures which resulted in an excellent inter- and intra-observer reproducibility, as reflected by the very high correlation coefficients.

The quantitative hybrid microSPECT-CT approach allows for the noninvasive analysis of both proximal and distal murine hindlimbs, although we have identified potential limitations related to intense bladder activity, which may reduce the reliability of the analysis from the proximal hindlimb located above the site of ligation of the femoral artery. The scatter of activity from the bladder resulted in a variable overestimation of counts in the proximal hindlimb estimated from the microSPECT-CT images. Although aspiration of radioactivity from the bladder improved our analysis of proximal sections, this solution may not be ideal for serial imaging of the same animal over prolonged period of time, because of the potential risk for infection. In spite of this limitation for estimation of angiogenesis in proximal hindlimb segments, there was an almost perfect observer-independent reproducibility of the image analysis, which strongly correlated with the gamma well counting in the distal segments. This noninvasive microSPECT-CT imaging approach holds great promise for

assessment of both spatial and temporal changes in peripheral angiogenesis in animals following ischemic injury and for the evaluation of therapeutic intervention.

To further demonstrate the applicability of this quantitative targeted αv integrin microSPECT-CT imaging approach for *in vivo* serial assessment of angiogenesis, we evaluated two strains of mice with known differences in their angiogenic response following ischemic injury. Serial microSPECT-CT images were acquired in eNOS knockout mice lacking endothelial nitric oxide which is a crucial mediator of angiogenesis. The mice lacking eNOS have been previously shown to have decreased peripheral angiogenesis in response to ischemia, and significantly impaired flow recovery in the distal hindlimb as determined using highly invasive techniques including deep penetrating laser Doppler imaging and histological analysis.¹ In the current study, eNOS knockout and control mice were serially imaged at baseline and at 1 and 4 weeks after surgical resection of right femoral artery which resulted in severe ischemia using the same imaging protocol as in validation experiments. As expected we observed a significant increase of ^{99m}Tc-NC100692 retention within ischemic distal limb in both animal groups at 1 week post ligation, which normalized by 4 weeks. The analysis of serial microSPECT-CT images revealed that there is a statistically significant ($P < 0.05$) reduction in relative ^{99m}Tc-NC100692 retention in eNOS knockouts at 1 week from the surgery suggesting impaired peripheral angiogenesis in these knockout mice. These differences between the groups normalized at 4 week post ligation. The observed differences between the groups obtained using noninvasive quantitative analysis of targeted microSPECT-CT ^{99m}Tc-NC100692 imaging were in good agreement with those obtained using more invasive techniques previously published by our group.¹ These invasive techniques included immunohistochemistry of microscopic sections, Western Blotting, and Doppler-laser to assess perfusion. All of these approaches required irreversible destruction of biopsied sample or significant surgical insult making serial evaluations non-feasible.

In conclusion, we have developed a reproducible and accurate approach for semi-automated analysis of microSPECT-CT images for quantitative evaluation of angiogenesis, which is applicable to murine models of ischemia-induced peripheral angiogenesis. The analysis approach has been carefully validated and is now freely available online (<http://www.bioimagesuite.org/>) as a user-friendly image analysis tool. This hybrid targeted imaging approach would be potentially applicable for evaluation of other biological processes in animals, using a wide range of potential targeted radiotracers for microSPECT-CT or microPET-CT imaging. Although this image analysis approach was designed to analyze murine microSPECT-CT images, the approach also holds promise for future clinical translational studies involving *in vivo* imaging of angiogenesis and other biological processes in patients with peripheral arterial disease.

Acknowledgments

Financial support: This work was supported in part by the NIH under grants R01HL065662 (AJS), R01EB006494 (XP) and Juvenile Diabetes Research Foundation grant # 10-2006-726 (LWD).

References

1. Yu J, deMuinck ED, Zhuang Z, et al. Endothelial nitric oxide synthase is critical for ischemic remodeling, mural cell recruitment, and blood flow reserve. *Proc Natl Acad Sci U S A*. Aug 2; 2005 102(31):10999–11004. [PubMed: 16043715]
2. Cai W, Chen K, Mohamedali KA, et al. PET of vascular endothelial growth factor receptor expression. *J Nucl Med*. Dec; 2006 47(12):2048–2056. [PubMed: 17138749]
3. Chen X, Sievers E, Hou Y, et al. Integrin alpha v beta 3-targeted imaging of lung cancer. *Neoplasia*. Mar; 2005 7(3):271–279. [PubMed: 15799827]

4. Collingridge DR, Carroll VA, Glaser M, et al. The development of [(124)I]iodinated-VG76e: a novel tracer for imaging vascular endothelial growth factor in vivo using positron emission tomography. *Cancer Res.* Oct 15; 2002 62(20):5912–5919. [PubMed: 12384557]
5. Hua J, Dobrucki LW, Sadeghi MM, et al. Noninvasive imaging of angiogenesis with a 99mTc-labeled peptide targeted at alphavbeta3 integrin after murine hindlimb ischemia. *Circulation.* Jun 21; 2005 111(24):3255–3260. [PubMed: 15956134]
6. Li S, Peck-Radosavljevic M, Kienast O, et al. Iodine-123-vascular endothelial growth factor-165 (123I-VEGF165). Biodistribution, safety and radiation dosimetry in patients with pancreatic carcinoma. *Q J Nucl Med Mol Imaging.* Sep; 2004 48(3):198–206. [PubMed: 15499293]
7. Lu E, Wagner WR, Schellenberger U, et al. Targeted in vivo labeling of receptors for vascular endothelial growth factor: approach to identification of ischemic tissue. *Circulation.* Jul 8; 2003 108(1):97–103. [PubMed: 12821549]
8. Bach-Gansmo T, Danielsson R, Saracco A, et al. Integrin receptor imaging of breast cancer: a proof-of-concept study to evaluate 99mTc-NC100692. *J Nucl Med.* Sep; 2006 47(9):1434–1439. [PubMed: 16954550]
9. Edwards D, Jones P, Haramis H, et al. 99mTc-NC100692--a tracer for imaging vitronectin receptors associated with angiogenesis: a preclinical investigation. *Nucl Med Biol.* Apr; 2008 35(3):365–375. [PubMed: 18355693]
10. Indrevoll B, Kindberg GM, Solbakken M, et al. NC-100717: a versatile RGD peptide scaffold for angiogenesis imaging. *Bioorg Med Chem Lett.* Dec 15; 2006 16(24):6190–6193. [PubMed: 17000103]
11. Kenny LM, Coombes RC, Oulie I, et al. Phase I trial of the positron-emitting Arg-Gly-Asp (RGD) peptide radioligand 18F-AH111585 in breast cancer patients. *J Nucl Med.* Jun; 2008 49(6):879–886. [PubMed: 18483090]
12. Hua J, Bourke B, Song J, et al. Noninvasive detection of angiogenesis, with a technetium-99m labeled peptide targeted at alpha v beta 3 integrin following hindlimb ischemia. *J Am Col Cardiol.* 2004; 43(5):25A.
13. Dobrucki LW, Sinusas AJ. Molecular imaging. A new approach to nuclear cardiology. *Q J Nucl Med Mol Imaging.* Mar; 2005 49(1):106–115. [PubMed: 15724140]
14. Dobrucki LW, Sinusas AJ. Molecular cardiovascular imaging. *Curr Cardiol Rep.* Mar; 2005 7(2): 130–135. [PubMed: 15717960]
15. Dobrucki LW, Sinusas AJ. Cardiovascular molecular imaging. *Semin Nucl Med.* Jan; 2005 35(1): 73–81. [PubMed: 15645396]
16. Sinusas AJ. Imaging of angiogenesis. *J Nucl Cardiol.* Sep-Oct;2004 11(5):617–633. [PubMed: 15472646]
17. Hua J, Bourke BN, Song J, et al. Noninvasive detection of angiogenesis, with a technetium-99m labeled peptide targeted at alpha v beta 3 integrin following hindlimb ischemia. *Journal Of The American College Of Cardiology.* Mar 3; 2004 43(5):25A–25A.

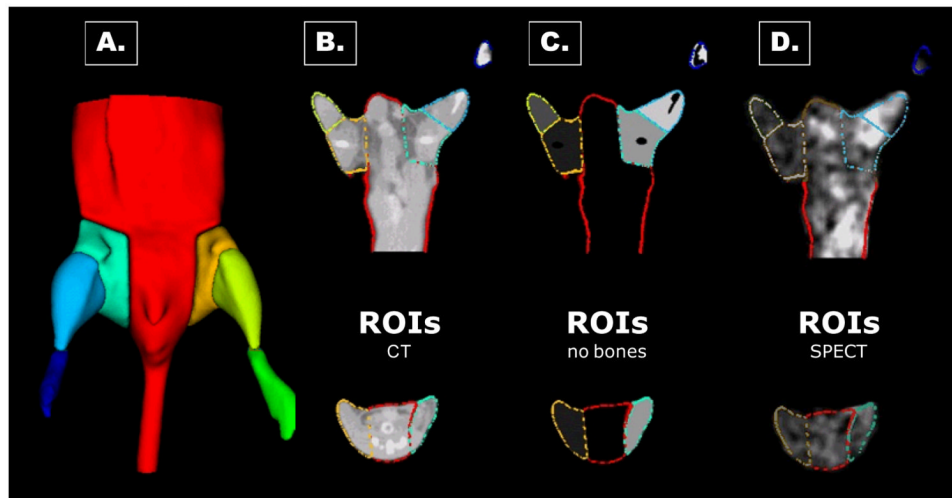


Figure 1. Method for analysis of microSPECT-CT images

Planes were interactively positioned over the lower body of mice to segment the microCT to generate multiple volumes-of-interest (VOIs) (A). The contours of these VOIs are illustrated superimposed on a representative microCT image (B). K-means clustering-based segmentation was performed to eliminate bones from the VOIs (C). This complex irregular objectmap was applied to the registered microSPECT images to determine mean counts in each VOI (D).

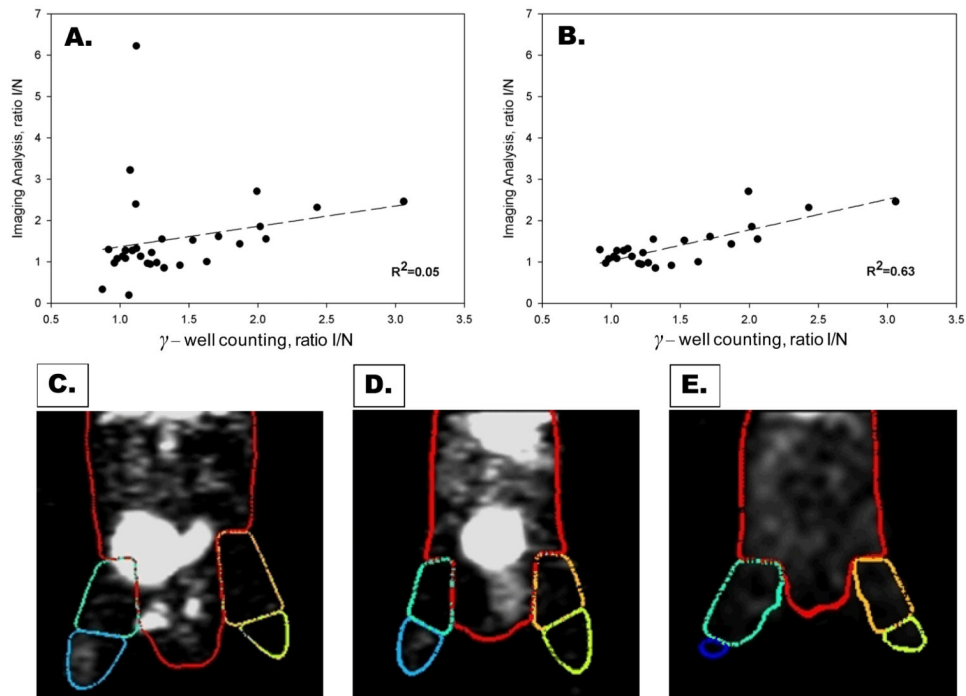


Figure 2. Validation of microSPECT-CT image analysis approach

Correlation between ischemic-to-nonischemic (I/N) ratios of counts calculated from image analysis and gamma well counting for both proximal and distal regions (A). The correlation was poor ($R^2=0.05$) when all proximal and distal regions were included (A). The correlation coefficient between imaging analysis and gamma well counting improved significantly ($R^2=0.63$) after proximal regions contaminated with scatter from radioactivity in the bladder have been removed from the analysis (B). Shown below are representative ^{99m}Tc -NC100692 microSPECT-CT images from three mice at 7 days after surgical ligation of right femoral artery with superimposed VOIs. Figure 2 C illustrates a mouse with radioactivity within bladder which falls within the right proximal VOI, resulting in overestimation of counts in ischemic (right) relative to non-ischemic (left) proximal leg. Figure 2 D illustrates a second mouse with bladder located centrally in the body and no significant contamination of proximal hindlimb VOIs. Figure 2E illustrates images from third mouse following removal of the radioactive urine from the bladder by needle aspiration immediately before SPECT acquisition.

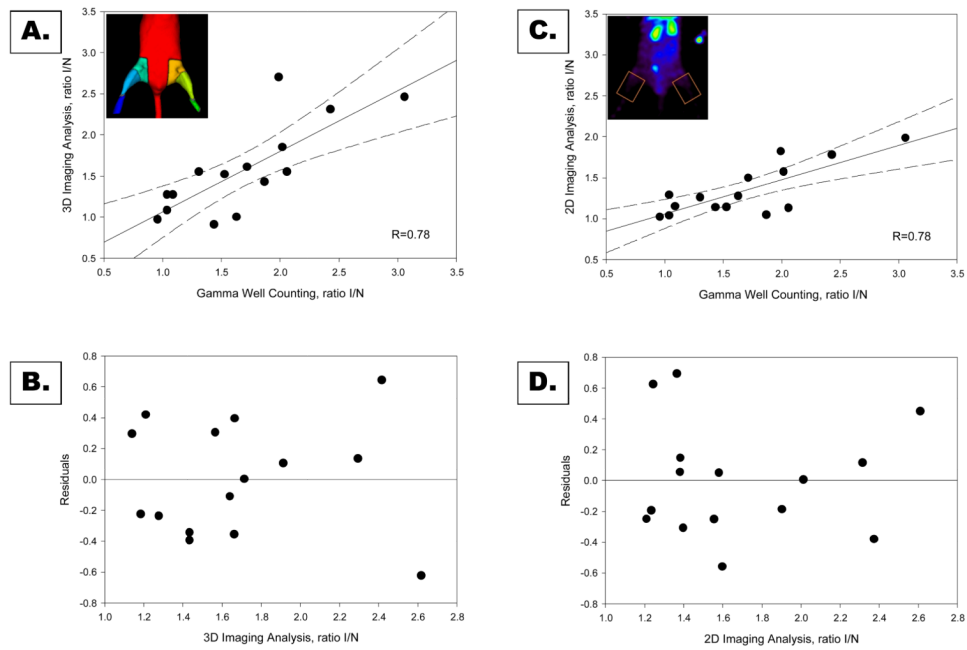


Figure 3. Validation of analysis of distal hindlimb

There was a good correlation ($R=0.78$) between ischemic-to-nonischemic counts ratio calculated from 3D volumetric analysis of microSPECT-CT images (A), and 2D analysis of maximum projection images (C) relative to gamma well counting for the distal hindlimb. Linear correlation (solid line) and 95% confidence intervals (dashed line) are shown (B & D). The quality of the fit was confirmed by residuals plot for microSPECT-CT images (B), 2D maximum projection images (D) analysis approaches.

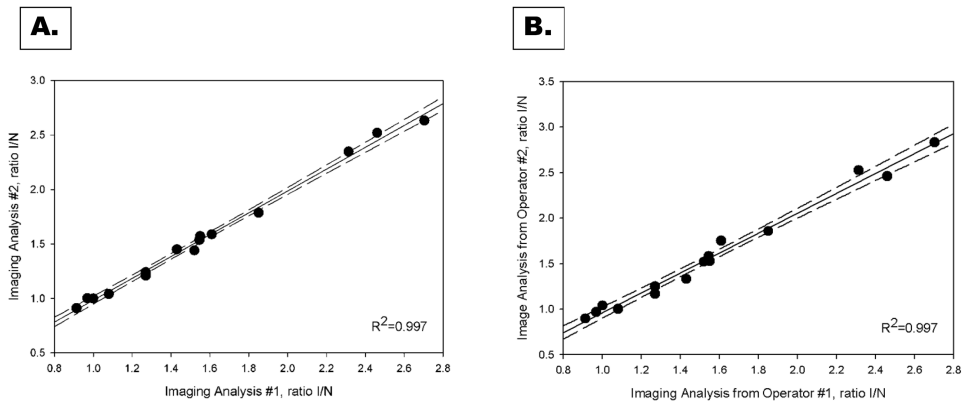


Figure 4. Reproducibility of image quantification

The intra-observer (A) and inter-observer (B) reproducibility of microSPECT-CT image analysis were excellent.

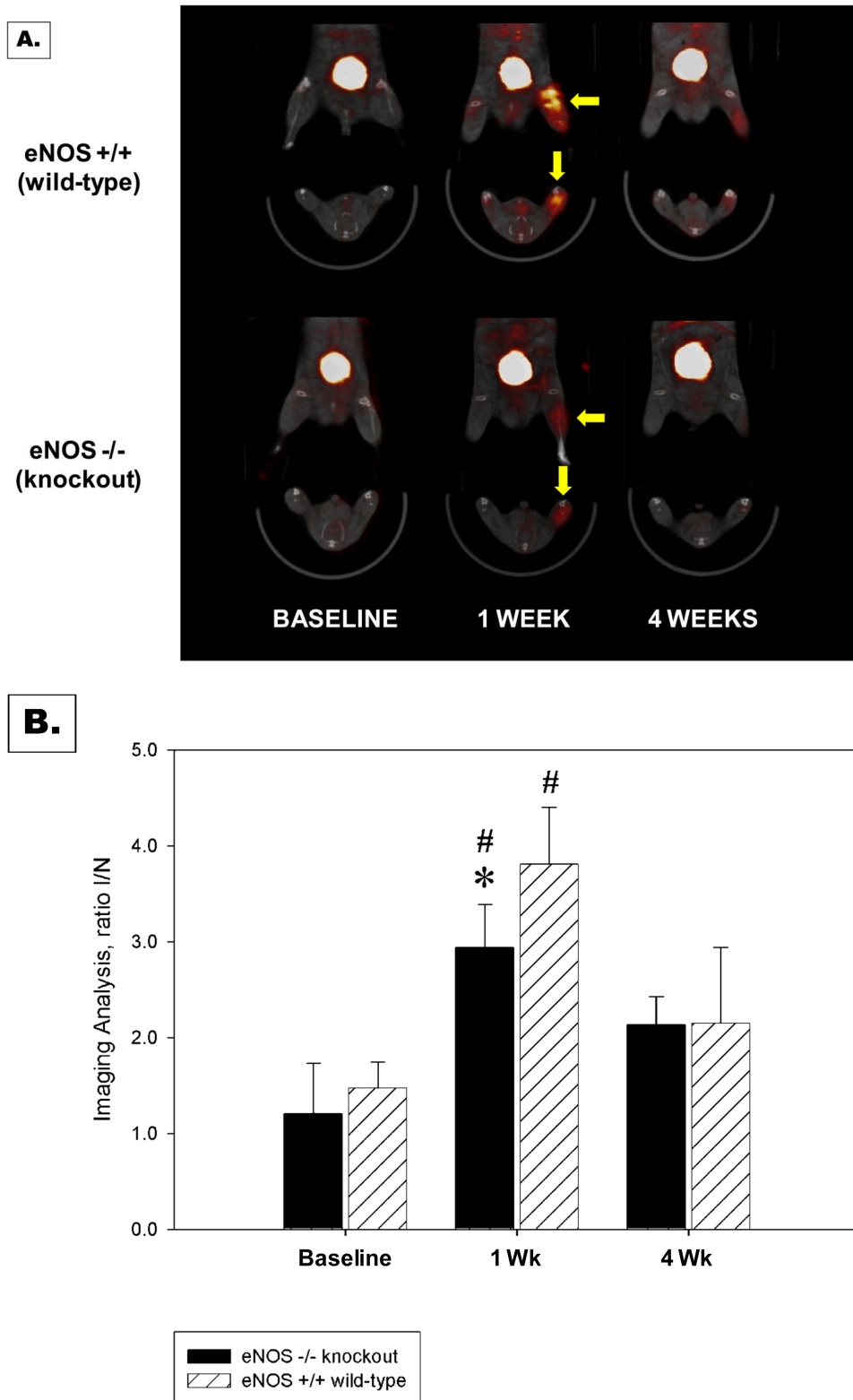


Figure 5. Analysis of wild-type and eNOS knockout mice
 Representative microSPECT-CT images of wild-type (eNOS^{+/+}) and eNOS-knockout (eNOS^{-/-}) mice injected with ^{99m}Tc-NC100692 at baseline, 7 days, and 4 weeks post right

femoral artery ligation (A). Yellow arrows indicate ischemic regions with increased ^{99m}Tc -NC100692 retention. Less retention is seen in eNOS $^{-/-}$ mice. Serial microSPECT-CT images were analyzed and I/N ^{99m}Tc -NC100692 activity ratios calculated (B). There was a significant ($P < 0.05$) increase of ^{99m}Tc -NC100692 retention in ischemic leg at 7 days post surgery in both groups. However, there was significantly less retention in the eNOS $^{-/-}$ mice at 7 days compared with wild-type mice.

* $P < 0.05$ vs. wild-type

$P < 0.05$ vs. baseline